







FREEZING PATTERNS IN SALINE SOILS: MODELING WITH REGARD TO THE OSMOTIC EFFECT

M. M. Ramazanov^{1,2} , N. S. Bulgakova^{1,*} , L. I. Lobkovsky^{3,4} , E. M. Chuvilin^{4,5} ,
S. R. Gadzhimagomedova¹ , and N. E. Shakhova^{2,4,6} 

¹Institute for Geothermal Research and Renewable Energy, Branch of Joint Institute for High Temperatures, Russian Academy of Sciences, Makhachkala, Russia

²Sadovsky Institute of Geosphere Dynamics, Russian Academy of Sciences, Moscow, Russia

³P. P. Shirshov Institute of Oceanography, Russian Academy of Sciences, Moscow, Russia

⁴Science Department, Tomsk State University, Tomsk, Russia

⁵Skolkovo Institute of Science and Technology (Skoltech), Innovation Center Skolkovo, Moscow, Russia

⁶V. I. Il'ichev Pacific Oceanological Institute, Far Eastern Branch Russian Academy of Sciences, Vladivostok, Russia

* **Correspondence to:** Natalia S. Bulgakova, ipgnatali@mail.ru

Abstract: Freezing patterns in a porous soil saturated with a saline solution are investigated with regard to osmotic effects, using a model suggested previously by the authors but in a more general formulation. The results include a numerical and an approximate self-similar analytical solution to a nonlinear problem; description of typical freezing behavior in the presence of osmotic pressure. The modeling results agree well with experimental evidence on freezing of saline clay and sand. The model includes three porous domains with ice (I), thermodynamically equilibrated ice+solution (II), and a liquid saline solution (III) in the pores. The modeling is performed for a simplified case of domains II and III that share a mobile phase boundary where the solution freezes up partially, with heat release.

Keywords: freezing, saline rock, osmosis, mathematical model, modeling, physical model.

Citation: Ramazanov, M. M., N. S. Bulgakova, L. I. Lobkovsky, E. M. Chuvilin, S. R. Gadzhimagomedova, and N. E. Shakhova (2024), Freezing Patterns in Saline Soils: Modeling with Regard to the Osmotic Effect, *Russian Journal of Earth Sciences*, 24, ES4008, EDN: HICJYC, <https://doi.org/10.2205/2024es000919>

1. Introduction

Freezing of rocks and soils saturated with a solution of salts is a complex process involving different mechanisms for salt and moisture transport, as well as stress and strain dynamics in the mineral skeleton. Since the process of freezing saline soil depends nonlinearly on many factors, the identification of patterns is significantly complicated. It can be investigated on the basis of the mathematical model previously proposed by the authors [Ramazanov et al., 2023], but in a more general formulation, and compare the results with data from physical and field experiments [Chuvilin, 1999; Chuvilin et al., 1998; Ershov et al., 1997]. The correlation between the transport of salt and moisture in freezing saline soils was studied in [Chuvilin et al., 1998]. The results of physical experiments reported in [Chuvilin, 1999] were used to study the behavior of ions in freezing and thawing soils, and in ice. The available evidence relevant to freezing also includes interactions of frozen soil with saline solutions. In [Ershov et al., 1997], processes associated with different types of interactions between liquid brine and frozen rocks are considered.

According to the present views, the Siberian Arctic shelf underwent repeated freezing and thawing associated with regression and transgression events, which produced permafrost with numerous lenses of brines at negative temperatures called cryopegs [Dubikov and Ivanova, 1990; Streletskaaya and Leibman, 2002]. It is noted in [Dubikov and Ivanova, 1990] that frozen saline soils by many of its properties occupy a position between frozen

RESEARCH ARTICLE

Received: 17 April 2024

Accepted: 12 July 2024

Published: 13 November 2024



Copyright: © 2024. The Authors. This article is an open access article distributed under the terms and conditions of the Creative Commons Attribution (CC BY) license (<https://creativecommons.org/licenses/by/4.0/>).

and unfrozen soils. They contain more unfrozen water than the same frozen soils. It determines their peculiarity together with other features of their composition and structure. In [Streletskaia and Leibman, 2002], the actual material is considered from the point of view of the formation of cryopegs as residual brines during the formation of ice deposits.

One of possible reason for current climate change in the Arctic is considered to be the formation and release a lot of methane due to subaquatic permafrost degradation, as methane is a potent greenhouse gas. Saline seawater and cryopegs contribute largely to permafrost degradation and the ensuing emission of methane released by dissociating metastable methane hydrates self-preserved in frozen rocks [Chuvilin et al., 2019; Lobkovskii and Ramazanov, 2018; Shakhova et al., 2017; Yakushev, 2009]. The rate of submarine permafrost degradation and the emergence of gas migration pathways are key factors controlling methane emissions on the East Siberian Arctic shelf [Shakhova et al., 2017].

The process of permafrost degradation and the reverse process of salt rock freezing have the same transport mechanism – osmotic filtration (moisture migration). Osmosis can lead to abnormally high pressures capable of destroying frozen rocks [Berry and Hanshaw, 1960; Marine and Fritz, 1981]. Thus, developing model can easily describe the degradation of permafrost rocks containing accumulations of gas hydrates and free gas under the influence of solutions and the associated osmotic effect.

There exist various models of freezing and thawing processes in saline rocks and soils [Maksimov and Tsyppkin, 1987; Tsyppkin, 2009; Vasiliev et al., 1996], but our model is advantageous by including osmosis. The osmotic motion of water molecules driven by the solute concentration gradient is a powerful mechanism of mass transport in low-permeable porous media [Ramazanov et al., 2019, 2022]. This modeling approach can be used to determine a mathematical criterion for the formation of cryopegs in freezing saline soils, which depends largely on the osmotic filtration [Ramazanov et al., 2023]. Another advantage of our model is in due regard for deformation of the host rocks, given that osmotic pressure can cause rock failure.

In this paper using the model proposed in [Ramazanov et al., 2023] by numerical and analytical methods, we investigate the processes of freezing of rocks and soils saturated with salt solution, taking into account the osmotic force.

2. Problem Formulation

The model simulates permeable soil saturated with a saline solution of a constant concentration, at a certain temperature. At some moment of time, the temperature of the model top falls below the freezing point at given local pressure and salt concentration values. Thereby two freezing fronts arise and propagate downward (Figure 1): the boundaries between domains I and II (fully and partly frozen domains, with pore ice and ice + saline solution in thermodynamic equilibrium, respectively), and between partly frozen (II) and unfrozen (III) domains. The modeling investigates the patterns of evolution of the multi-phase system with regard to the osmotic effect and deformation of the host rock and compares the results with experimental data.

3. Mathematical Model

A detailed description of the equations in each domain, the boundary conditions, and their transformations are given in the previous paper [Ramazanov et al., 2023] published in this journal. Here, we present these equations immediately in dimensionless and self-similar form [Ramazanov et al., 2023].

The pressure is counted from the hydrostatic level, and the temperature from level T^0 . To make them dimensionless, let's introduce the following scales:

$$\begin{aligned} [z] = h, \quad [v] = -\frac{k}{\eta h} \frac{dP}{dT} (T_0 - T^0), \quad [t] = \frac{h}{[v]}, \quad [T] = T_0 - T^0, \\ [p] = -\frac{dP}{dT} (T_0 - T^0), \quad [c] = c_0, \end{aligned} \quad (1)$$

where k is the permeability; v is the field of the solution velocity; T is the temperature; p is the pressure; c is the concentration; c_0 is the characteristic concentration; η is the solution viscosity; h is the domain thickness; T_0 is the temperature at the lower boundary of domain III, T^0 is the temperature at the boundary $z = z_1$.

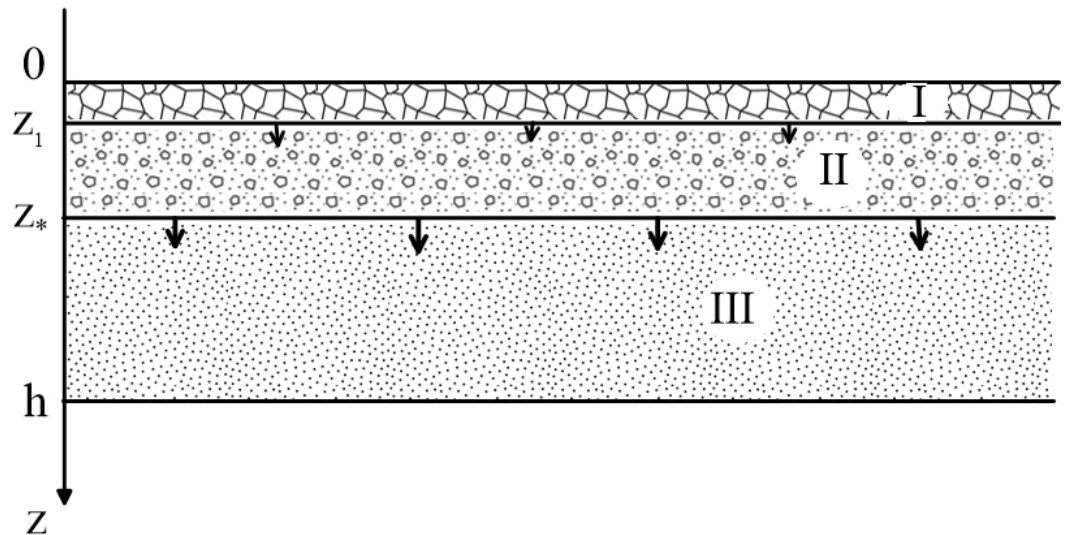


Figure 1. Problem sketch: I – ice-saturated frozen domain; II – partly frozen domain saturated with thermodynamically equilibrated ice and saline solution; III – unfrozen domain saturated with liquid saline solution; $z = z_1(t)$ is the mobile boundary of domain I; $z = z_*(t)$ is the front of partial freezing.

4. Self-Similar Problem Formulation and Solution

The solution is sought in the self-similar form, with the new coordinate ξ

$$v = \frac{v(\xi)}{\sqrt{t}}, \quad T = T(\xi), \quad c = c(\xi), \quad p = p(\xi), \quad \xi = \frac{z}{\sqrt{t}}. \tag{2}$$

Then, different domains will be described as follows:

Frozen Domain (I)

$$-\frac{\xi}{2} \frac{dT_i}{d\xi} = \frac{1}{Pe_{T_i}} \frac{d^2T_i}{d\xi^2}. \tag{3}$$

Partly Frozen Domain (II)

$$\begin{aligned} v &= s \left[(\gamma_f + \psi_0) \frac{dc}{d\xi} + \frac{dT}{d\xi} \right]; \\ -\frac{\xi}{2N_s} \frac{ds}{d\xi} + \frac{\xi}{2N_p} \left(\frac{dT}{d\xi} + \psi_0 \frac{dc}{d\xi} \right) + \frac{dv}{d\xi} &= 0; \\ -\left(\frac{\gamma_c \xi}{2} - v \right) \frac{dc}{d\xi} &= \frac{1}{Pe_c} \frac{d^2c}{d\xi^2} + \frac{\gamma_s \xi}{2} \frac{ds}{d\xi}; \\ -\left(\frac{\gamma_T \xi}{2} - v \right) \frac{dT}{d\xi} &= \frac{1}{Pe_T} \frac{d^2T}{d\xi^2} + \frac{\gamma_q \xi}{2} \frac{ds}{d\xi}. \end{aligned} \tag{4}$$

Unfrozen Domain (III)

$$\begin{aligned}
 v &= -\frac{dp}{d\xi} + \gamma_f \frac{dc}{d\xi}; \\
 -\frac{\xi}{2N_{p0}} \frac{dp}{d\xi} &= \frac{d^2p}{d\xi^2} - \gamma_f \frac{d^2c}{d\xi^2}; \\
 -\left(\frac{\gamma_c \xi}{2} - v\right) \frac{dc}{d\xi} &= \frac{1}{s_0 Pe_c} \frac{d^2c}{d\xi^2}; \\
 -\left(\frac{\gamma_T \xi}{2} - v\right) \frac{dT}{d\xi} &= \frac{1}{Pe_T} \frac{d^2T}{d\xi^2}.
 \end{aligned}
 \tag{5}$$

where Pe_T, Pe_c are, respectively, the temperature and concentration Péclet numbers.

$$\begin{aligned}
 \frac{1}{N_s} &= m \left(1 - \frac{\rho_i}{\rho_w}\right), \quad \frac{1}{N_{p0}} = \frac{1}{m_0} \left[\frac{\partial m}{\partial p} + \frac{m_0}{\rho_w} \frac{\partial \rho_w}{\partial p} \right] (T_0 - T^0) \left| \frac{dP}{dT} \right|, \\
 \frac{1}{N_p} &= \left[\left(s_0 + (1 - s_0) \frac{\rho_i}{\rho_w} \right) \frac{\partial m}{\partial p} + \frac{m}{\rho_w} \left(s_0 \frac{\partial \rho_w}{\partial p} + (1 - s_0) \frac{\partial \rho_i}{\partial p} \right) \right] (T_0 - T^0) \left| \frac{dP}{dT} \right|, \\
 \gamma_f &= \rho_w \left| \frac{\partial \mu_1}{\partial c} \right| c_0 \left[(T_0 - T^0) \left| \frac{dP}{dT} \right| \right]^{-1}, \quad \gamma_T = \frac{C_m + m s \beta_w \bar{T} \left| \frac{dP}{dT} \right|}{\rho_w C_w + \beta_w \bar{T} \left| \frac{dP}{dT} \right|}, \\
 \gamma_q &= \frac{qm\rho_i}{\left[\rho_w C_w + \beta_w \bar{T} \left| \frac{dP}{dT} \right| \right] (T_0 - T^0)}, \quad \gamma_c = s_0(m + \Gamma), \quad \gamma_s = m \frac{\rho_i}{\rho_w} + \Gamma, \\
 \Gamma(K, c) &= \frac{\partial a(K, c)}{\partial c}, \quad \lim_{K \rightarrow \infty} a(K, c) = a_\infty, \\
 Pe_T &= \frac{[v]h \left[\rho_w C_w + \beta_w \bar{T} \left| \frac{dP}{dT} \right| \right]}{\lambda_m}, \quad Pe_c = \frac{[v]h}{ms_0 D}, \quad [v] = -\frac{k}{\eta h} \frac{dP}{dT} (T_0 - T^0).
 \end{aligned}$$

where s_0 is the characteristic water saturation in domain II; ρ_w, ρ_i are densities of water and ice, respectively; T_i is the ice temperature; C_m is the effective heat capacity per unit volume of an saturated porous soil; C_w, C_i, C_s are, respectively, the heat capacity of water, ice and soil; λ_m is the effective thermal conductivity of an saturated porous soil; $\lambda_w, \lambda_i, \lambda_s$ are, respectively, the thermal conductivity of water, ice and soil; μ_1 is the chemical potential of solvent; D is the salt diffusion coefficient; q is the specific heat of ice melting; β_w is the thermal expansion coefficient; m is the porosity; a is the concentration of salt in the solid phase of a porous medium; a_∞ the value of the maximum adsorption; K is the constant of the adsorption equilibrium; ψ_0 constant characterizing the degree of decrease in the freezing point of water due to the presence of dissolved salt.

Boundary Conditions

$$\xi = 0: \quad T_i = \frac{T_i^0 - T^0}{T_0 - T^0}, \tag{6}$$

$$\begin{aligned}
 \xi = \xi_1: \quad T_- = T_+ = 0, \quad \frac{1}{Pe_{T_i}} \frac{dT_-}{d\xi} &= \frac{\gamma_{qi} s^0}{2} \xi_1 + \frac{1}{Pe_T} \frac{dT_+}{d\xi}, \quad \gamma_{qi} = \frac{qm\rho_i}{\rho_w c_w (T_0 - T^0)}, \\
 s^0 \left(\frac{1}{s_0 Pe_c} \frac{dc_+}{d\xi} + \frac{\rho_i}{\rho_w} \frac{m \xi_1}{2} c_+ \right) &= 0, \quad v_+ = s^0 \left(1 - \frac{\rho_i}{\rho_w} \right) \frac{m \xi_1}{2},
 \end{aligned}
 \tag{7}$$

$$\begin{aligned} \xi = \xi_* : \quad v_- - \frac{m}{2} s_* \xi_* - \frac{\rho_i m}{2 \rho_w} (1 - s_*) \xi_* &= v_+ - \frac{m}{2} \xi_*, \\ T_- = T_+ = T_*, \quad -\gamma_q (1 - s_*) \frac{1}{2} \xi_* + \frac{1}{Pe_T} \frac{dT_-}{d\xi} &= \frac{1}{Pe_T} \frac{dT_+}{d\xi} \\ c_- = c_+ = c_*, \quad -\gamma_s (1 - s_*) \frac{c_*}{2} \xi_* + \frac{s_*}{s_0 Pe_c} \frac{dc_-}{d\xi} &= \frac{1}{s_0 Pe_c} \frac{dc_+}{d\xi} \end{aligned} \tag{8}$$

$$\xi \rightarrow \infty : \quad p \rightarrow p_0, \quad T \rightarrow 1, \quad c \rightarrow 1, \tag{9}$$

where s^0 is the water saturation at the boundary $\xi = \xi_1$ between domains I (pore ice) and II (equilibrated pore ice + solution). The subscripts and superscripts have the following meaning: subscripts + and - refer to values approaching the boundaries from below and from above, respectively; subscript * indicates the value at the boundary $\xi = \xi_*$, superscript 0 - at the boundary $\xi = \xi_1$, subscript 0 - at the boundary $\xi \rightarrow \infty$ or the characteristic value of the parameter.

With the given parameters T_i^0, T_0, c_0, p_0 and s^0 , the sought parameters are: mobile phase boundaries ξ_1, ξ_* , temperature in frozen domain I; temperature, salt concentration, and water saturation in partly frozen domain II and at its boundaries; temperature, salt concentration, and pressure in unfrozen domain III. Note that the boundaries in self-similar coordinates also define the propagation rates of the respective fronts.

Equations (2-9) in the self-similar formulation make up a closed model that simulates freezing of saline soil with regard to osmosis as a driving force. In initial coordinates the model is detailed in [Ramazanov et al., 2023]. In the general case, the model is quite sophisticated, as it contains two moving phase transition boundaries. We consider the particular case when the frozen domain (I) can be neglected. In [Ramazanov et al., 2023], a condition is given under which, as a first approximation, an ice layer can be neglected. It is possible if the front between domains I and II propagates much more slowly than that between II and III, i.e.

$$\xi_1 \ll \xi_*. \tag{10}$$

Then we obtain

$$k \gg m \left(1 - \frac{\rho_i}{\rho_w} \right)^2 \frac{\lambda_{m_i}}{\rho_i q} \frac{\eta}{\beta_p (p_* - p_0)^2} (T^0 - T_i^0) \sim 10^{-18} (10 \div 10^{-1}) \tag{11}$$

In the conditions considered in this article, inequality (11) holds for permeability $k \sim 10^{-18} \div 10^{-17} m^2$ and more. This permeability corresponds to the Péclet numbers $Pe_T \sim 10^{-2} \div 10^{-1}$. On the other hand, osmotic properties are manifested for weakly permeable media (clay, silt, etc.), which are characterized by precisely such permeability and corresponding Péclet numbers. Therefore, the number $Pe_T = 0.1$ is taken as the base number in the calculations below.

Thus, inequality (11) is satisfied under the conditions under consideration, so domain I is excluded from further consideration. Unlike [Ramazanov et al., 2023], in this study, not only the second, but also the third domain is taken into account.

The boundary conditions in domains II and III, given that the origin of coordinates is at the base of domain I, which is immobile in this approximation, are

$$\xi = 0 : \quad T = 0, \quad (\gamma_f + \psi_0) \frac{dc}{d\xi} + \frac{dT}{d\xi} = 0, \tag{12}$$

$$\begin{aligned} \xi = \xi_* : \quad v_- - \frac{m}{2} s_* \xi_* - \frac{\rho_i m}{2 \rho_w} (1 - s_*) \xi_* &= v_+ - \frac{m}{2} \xi_*, \\ T_- = T_+ = T_*, \quad -\gamma_q (1 - s_*) \frac{1}{2} \xi_* + \frac{1}{Pe_T} \frac{dT_-}{d\xi} &= \frac{1}{Pe_T} \frac{dT_+}{d\xi}, \\ c_- = c_+ = c_*, \quad -\gamma_s (1 - s_*) \frac{c_*}{2} \xi_* + \frac{s_*}{s_0 Pe_c} \frac{dc_-}{d\xi} &= \frac{1}{s_0 Pe_c} \frac{dc_+}{d\xi}, \end{aligned} \tag{13}$$

$$\xi \rightarrow \infty: p \rightarrow p_0, T \rightarrow 1, c \rightarrow 1. \tag{14}$$

Thus, we have a system of equations (4–5) with boundary conditions (12–14). Since the model is nonlinear and generally has no analytical solution, one can take advantage of the fact that the Péclet number Pe_T of usually small, i.e. the filtration solution rate is much slower than the freezing rate (propagation of the freezing front). Then, the convective components in the transport equations can be neglected. The simplified model is still nonlinear because of generalized Darcy’s law (4), since the velocity is proportional to the product of water saturation by concentration and temperature gradients. However, it is possible to find an approximate solution assuming that water saturation s in the first equation of (4) is equal to some unknown average value \bar{s} . For the two remaining domains, the solution is as follows.

Partly Frozen Domain I (Pore Ice + Solution)

$$\begin{aligned} s - s^0 &= -s_T T - s_c (c - c^0), \\ c &= c^0 + C_1 \operatorname{erf}\left(\frac{\sqrt{\tilde{\alpha}_c}}{2} \xi\right) + \frac{Pe_c \gamma_s s_T}{\alpha_c - \tilde{\alpha}_T} C_3 \operatorname{erf}\left(\frac{\sqrt{\tilde{\alpha}_T}}{2} \xi\right), \\ T &= \frac{Pe_T \gamma_q s_c}{\alpha_T - \tilde{\alpha}_c} C_1 \operatorname{erf}\left(\frac{\sqrt{\tilde{\alpha}_c}}{2} \xi\right) + C_3 \operatorname{erf}\left(\frac{\sqrt{\tilde{\alpha}_T}}{2} \xi\right) \end{aligned} \tag{15}$$

where C_1, C_3 are determined from the boundary conditions at the moving phase interface $\xi = \xi_*$.

$$\begin{aligned} s_T &= \frac{\bar{s} Pe_T \gamma_T - \frac{1}{N_p}}{\frac{1}{N_s} + \bar{s} [Pe_T \gamma_q + (\gamma_f + \psi_0) Pe_c \gamma_s]}, \\ s_c &= \frac{\bar{s} (\gamma_f + \psi_0) Pe_c \gamma_c - \frac{\psi_0}{N_p}}{\frac{1}{N_s} + \bar{s} [Pe_T \gamma_q + (\gamma_f + \psi_0) Pe_c \gamma_s]}, \\ \tilde{\alpha}_c &= \frac{\alpha_T + \alpha_c + \sqrt{(\alpha_c - \alpha_T)^2 + 4 Pe_c \gamma_s s_T Pe_T \gamma_q s_c}}{2}, \\ \tilde{\alpha}_T &= \frac{\alpha_T + \alpha_c - \sqrt{(\alpha_c - \alpha_T)^2 + 4 Pe_c \gamma_s s_T Pe_T \gamma_q s_c}}{2}, \\ \alpha_T &= Pe_T \left(\gamma_T + \frac{N_s}{N_p} \gamma_q \right), \quad \alpha_c = Pe_c \gamma_c. \end{aligned} \tag{16}$$

We substitute the resulting solution for water saturation into the equation

$$\frac{1}{\xi_*} \int_0^{\xi_*} s(\xi, \bar{s}) d\xi = \bar{s} \tag{17}$$

and obtain a previously unknown value for the average water saturation \bar{s} .

Unfrozen Domain II (Pore Solution)

$$\begin{aligned} c &= 1 - (1 - c_*) \operatorname{erfc}\left(\frac{\sqrt{s_0 Pe_c \gamma_c}}{2} \xi\right) \Big/ \operatorname{erfc}\left(\frac{\sqrt{s_0 Pe_c \gamma_c}}{2} \xi_*\right), \\ T &= 1 - (1 - T_*) \operatorname{erfc}\left(\frac{\sqrt{Pe_T \gamma_c}}{2} \xi\right) \Big/ \operatorname{erfc}\left(\frac{\sqrt{Pe_T \gamma_c}}{2} \xi_*\right), \end{aligned} \tag{18}$$

$$p = p_0 + C_4 \operatorname{erfc} \left(\frac{\sqrt{\beta_{p_0}}}{2} \xi \right) + C_2 \operatorname{erfc} \left(\frac{\sqrt{s_0 P e_c \gamma_c}}{2} \xi \right), \tag{19}$$

$$v_p = \sqrt{\frac{\beta_{p_0}}{\pi}} C_4 e^{-\frac{\beta_{p_0}}{4} \xi^2} + \sqrt{\frac{s_0 P e_c \gamma_c}{\pi}} C_2 e^{-\frac{P e_c \gamma_c}{4} \xi^2} + \gamma_f \frac{dc}{d\xi}, \quad \beta_{p_0} = \frac{1}{N_{p_0}},$$

$$C_2 = \frac{-\gamma_f (1 - c_*) s_0 P e_c \gamma_c}{\beta_p - s_0 P e_c \gamma_c} \operatorname{erfc} \left(\frac{\sqrt{s_0 P e_c \gamma_c}}{2} \xi_* \right), \tag{20}$$

$$C_4 = p_* - p_0 - C_2 \operatorname{erfc} \left(\frac{\sqrt{s_0 P e_c \gamma_c}}{2} \xi_* \right) \operatorname{erfc} \left(\frac{\sqrt{\beta_{p_0}}}{2} \xi_* \right).$$

Estimating Moisture Content. If the moisture content density is expressed as the weight ratio of moisture (solid and liquid) to dry soil, then

$$W(\xi) = \begin{cases} m \rho_w \frac{1 - \left(1 - \frac{\rho_i}{\rho_w}\right) (1 - s) + \frac{\beta_p}{m} (1 - T - \psi_0 c)}{(1 - m) \rho_s}, & \xi \leq \xi_* \\ m \rho_w \frac{1 + \frac{\beta_{p_0}}{m} (p - p_0)}{(1 - m) \rho_s}, & \xi > \xi_* \end{cases}. \tag{21}$$

5. Results and Discussion

Thus, equations (15–21) provide a complete analytical solution to the nonlinear problem in the self-similar coordinates. The transitions to the initial coordinates and to the dimensional form are possible with equations (2) and (1), respectively.

The solution is valid at small Péclet numbers $Pe_T \ll 1$, which is commonly fulfilled. For the case of greater values, a forward numerical solution of problem (4–5) with boundary conditions (12–14) applied, taking into account convective transfer of heat and solutes. Furthermore, numerical modeling was used to check the analytical solution and proved its good accuracy.

In this problem of freezing saturated soils, two forces act: the force that pushes the solution into the unfrozen domain and the force that retracts the solution in the frozen domain. The pushing force arises due to equilibrium pressure increases with cooling and the water-ice density difference, while retracting force is due to the osmotic force. Depending on the values of the parameters, one or another force prevails.

Some results are illustrated in Figures 2–6.

Figure 2a–c shows patterns of partial freezing front propagation of solution depending on different parameters. With these parameter values, during the first 10 years, the freezing front moves at an average speed of about one meter per year, and then this speed decreases proportionally to $1/\sqrt{t}$. Curves in Figure 2a show that with an increase in the osmotic coefficient, the partial freezing front slows down, which is due to the difficulty of pushing the solution out by the freezing front. Figure 2b shows that as the Péclet number increases, the front moves faster because the rate of convective heat removal from the front increases. According to Figure 2c, as the water capacity of the soils increases, the front also moves faster, which is explained by the easier pushing of the solution into the unfrozen area.

Figure 3a–c shows depth-dependent water saturation distributions for water capacity β_p (a, b) and osmotic coefficient γ_f (a, c), two values each. Curves 1 and 2 correspond to the time $t = 1$ and 4 years, respectively. The curves above refer to the respective filtration solution rates.

Water saturation behind the freezing front decreases monotonically with time (Figure 3) as the soil is freezing up. Figure 3a shows that filtration solution rate is negative in this case, i.e., the solution is drawn from the thawed domain into the partly frozen domain by osmosis.

The pushing force predominates at lower β_p , other parameters being the same (Figure 3b), as well as at lower osmotic coefficients (Figure 3c). In Figure 3c, the osmotic

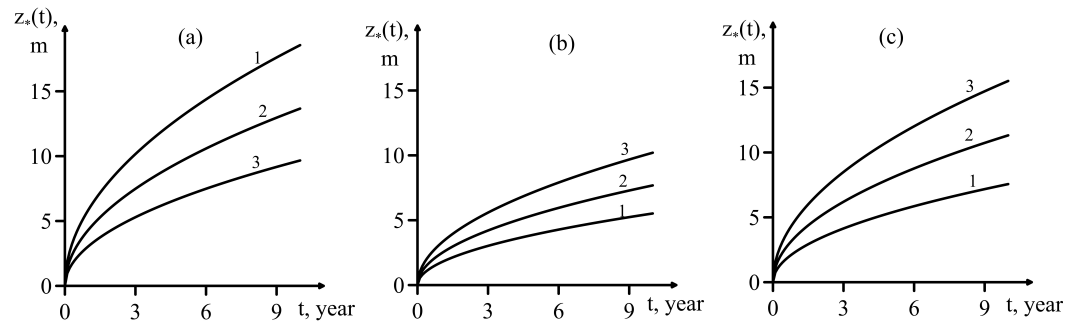


Figure 2. Time-dependent freezing propagation for different values of parameters at $c_0 = 0.8\%$, $T^0 = -2^\circ\text{C}$. (a): $Pe_T = 0.1$, $\beta_p = 0.1$, $\gamma_f = 0.27, 0.35, 1(1-3)$; (b): $\beta_p = 0.07$, $\gamma_f = 0.7$, $Pe_T = 0.01, 0.03, 0.3(1-3)$; (c): $Pe_T = 0.1$, $\gamma_f = 0.3$, $\beta_p = 0.01, 0.05, 0.1(1-3)$, where $\beta_p \equiv 1/N_p$ is the compressibility of the saturated porous soil (water capacity).

force coefficient is reduced compared to Figure 3a. As can be seen from the comparison, a decrease in osmotic force also leads to a predominance of the pushing force.

These results are quite consistent with the results of physical experiments [Chuvilin, 1999; Chuvilin et al., 1998], showing that clays in the considered freezing conditions draw the solution from the thawed area, and sands, on the contrary, are pushed out. At the same time, it is known that clays have semi-permeable and, consequently, osmotic properties [Kemper, 1961].

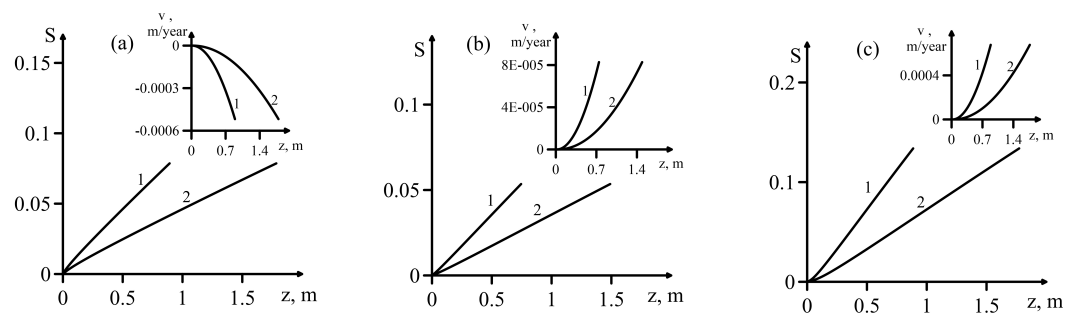


Figure 3. The distribution of water saturation for two time points (the filtration solution rate distributions are shown at the top) at: $Pe_c = 10$, $Pe_T = 0.1$, $c_0 = 1.7\%$, $T^0 = -2^\circ\text{C}$, $t = 1; 4$ year (1–2), where: $(\gamma_f, \beta_p) = (1, 0.03)$ (a); $(1, 0.01)$ (b); $(0.1, 0.03)$ (c).

Figure 4a–e shows the distributions of water saturation, velocity field, salt concentration, temperature, and pressure in the partially frozen domain after one year of freezing for two values of pore expansion coefficient β_p (water capacity) and two values of osmotic force coefficient. As you can see, in all cases, the qualitative properties of the distributions coincide, with the exception of the velocity field (Figure 4b). As the temperature increases with depth, water saturation increases at the account of partial melting, which leads to dilution (salt concentration decrease), while the equilibrium pressure decreases (Figure 4a, c–e).

It is pertinent to compare curves that represent different cases, using curves 1 as reference. Figure 4a shows that a decrease in water capacity (compressibility) led to a decrease in water saturation (curve 2), and a decrease in the osmosis coefficient can lead to both a decrease and an increase in water saturation, which explains the intersection of curves 3 and 1. These properties depend on the competition of two factors, the inflow (outflow) of the solution into the two-phase domain and the freezing of water (melting of ice). Curve 2 in Figure 4a is caused by both additional freezing of water (compared to curve 1) and outflow of solution (curve 2 in Figure 4b), and curve 3 is caused to competition between ice melting and moisture outflow (curve 3 in Figure 4b).

The concentration of salt is lower at lower compressibility but higher at lower osmotic coefficients (Figure 4c). To explain this effect, note first of all that the temperature patterns quite close for the three cases (Figure 4d). It follows from the thermodynamic equilibrium condition that lower salinity corresponds to higher pressure and vice versa, the temperature being constant [Ramazanov et al., 2023]. On the other hand, the pressure values are higher at lower compressibility and lower at lower osmotic coefficients (Figure 4e), which accounts for the patterns of Figure 4c.

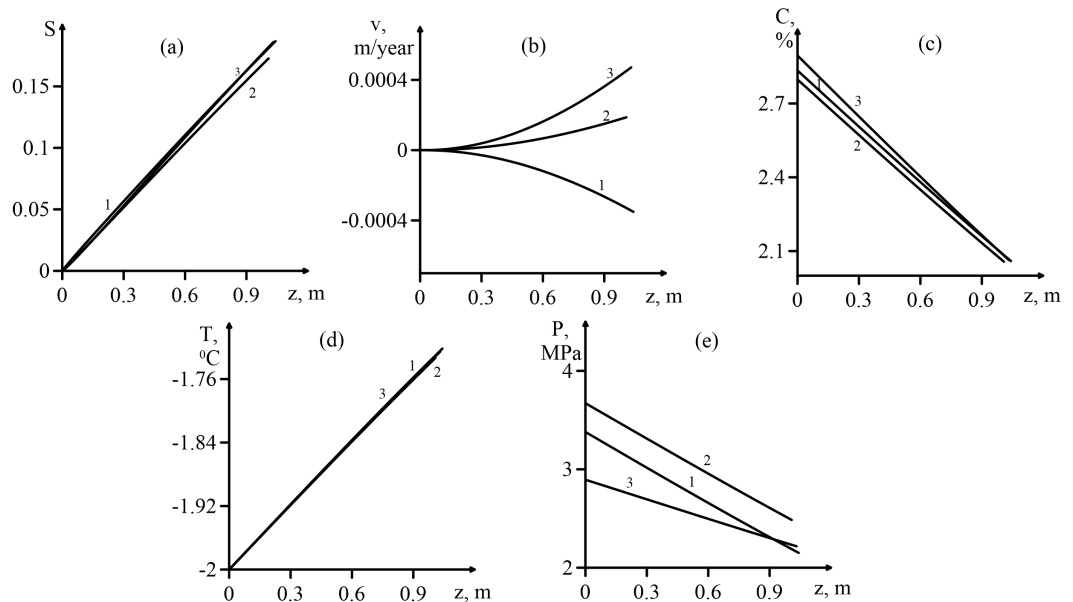


Figure 4. Water saturation (a), filtration solution rate (b), salt concentration (c), temperature (d), and pressure (e) in partly frozen domain a year after the onset of freezing, at $Pe_c = 10$, $Pe_T = 0.1$, $c_0 = 1.7\%$, $T^0 = -2^\circ\text{C}$, and $(\gamma_f, \beta_p = 1/N_p) = (0.1, 0.15)$ (1); $(0.1, 0.1)$ (2), $(0.05, 0.15)$ (3).

Figure 4 allows us to estimate the osmotic pressure gradient (osmotic force) under the considered freezing conditions. Consider the curves 1 in Figure 4. It follows from Figure 4b that in this case the solution is drawn from the thawed area into the frozen area. This means that the osmotic pressure gradient is greater than the pressure gradient shown in Figure 4e (curve 1) by the amount causing filtration of the solution. Based on Figure 4b and Darcy’s law, it can be shown that the pressure loss for filtration of the solution is small, i.e. the osmotic pressure gradient is approximately equal to the pressure gradient in Figure 4e (curve 1) and is approximately 1 MPa/m. On the other hand, it follows from Figure 4c (curve 1) that this gradient is caused by a salt concentration gradient of the order of $\nabla c_0 \sim 1\%/m = 10\text{g}/(\text{L} \cdot \text{m})$. If we take into account the complete dissociation of salt molecules into ions, then this gradient should be doubled. Thus, a salt concentration difference of the order of 10 g/L causes an osmotic pressure of the order of 1 MPa. This is in good agreement with theoretical and experimental estimates for shales [Neuzil, 2000].

Note that freezing rocks may have their own characteristics. Namely, near the cooled boundary, as ice forms, areas with a highly concentrated solution (cryopegs) may form. These areas, despite their relatively small size, can make a significant contribution to osmotic pressure. This effect can be taken into account using an effective osmotic coefficient, which can be several times higher than the corresponding coefficient for the thawed domain. In this regard, the values $\gamma_f \sim 1$ are also considered in [Ramazanov et al., 2023] and in this article. It should be noted that a more detailed study of the system of equations (4), with the separation of the boundary layer, allows theoretically calculating the specified effective osmosis coefficient, but goes beyond the scope of this study.

Figure 5 shows of moisture distribution in % of dry weight for different porous materials and different parameters. The upper panels present the results of physical experiments and the lower panels show calculations with the suggested model (4–5; 12–14).

The mathematical and physical modeling differed in temperature conditions on the top of the freezing domain: $-2\text{ }^{\circ}\text{C}$ and $-17\text{ }^{\circ}\text{C}$, respectively. Nevertheless, the theoretical (this study) and laboratory [Chuvilin, 1999; Chuvilin et al., 1998] results agree both qualitatively and quantitatively (Figure 5).

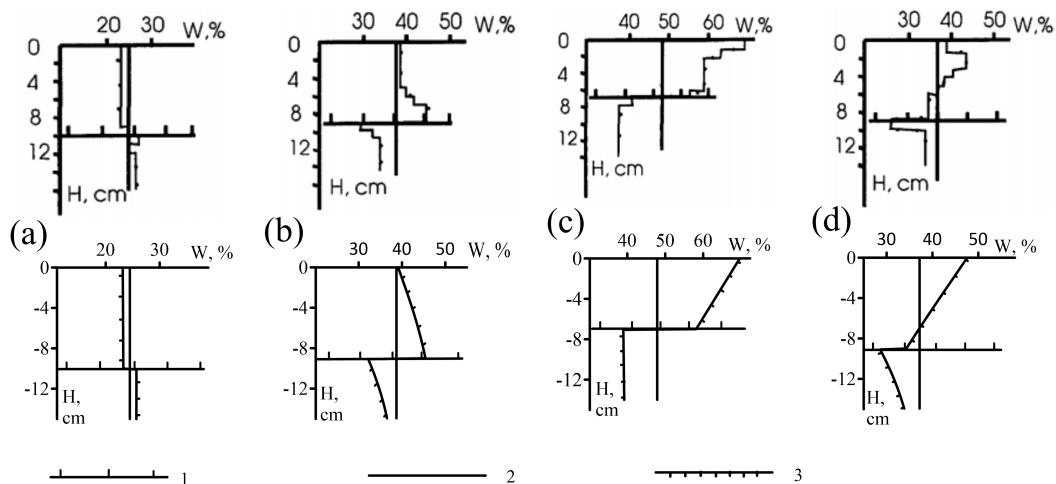


Figure 5. Depth-dependent moisture distribution, in % of dry weight W , according to physical modeling [Chuvilin, 1999] (upper panels) and calculations using equations (4–5, 12–14) of the suggested model (lower panels). In the experiment, soil samples: polymineral sand (a); polymineral clay (b); kaolinite clay, at pressures 0.2 MPa (c) and 1 MPa (d). Curve 1 – freezing front; 2 and 3 – initial and final moisture distribution in freezing soil, respectively.

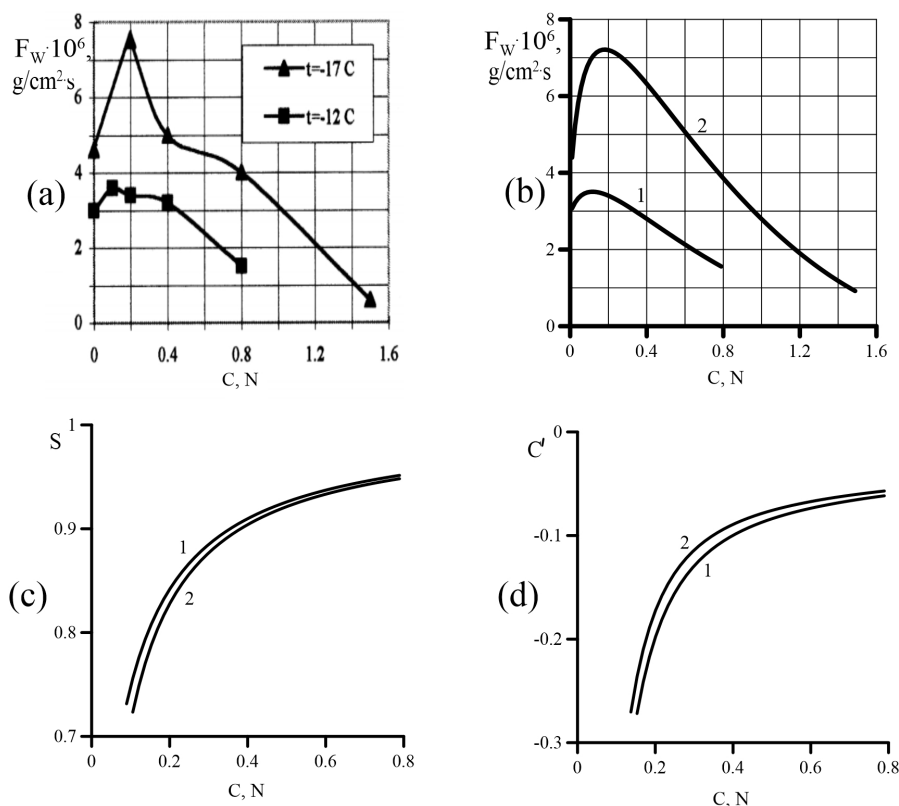


Figure 6. Average moisture expenditure F_w from unfrozen rock to partly frozen domain as a function of initial salinity C solution NaCl in freezing clay according to experiments (a) and modeling with suggested equations (b), and dependence of water saturation S and salinity gradient at the freezing front C' to salinity C calculated with the suggested model (c, d).

Depth-dependent moisture distribution patterns in freezing soils, obtained through mathematical modeling and experiments show the expulsion of pore moisture in wet saline sand, which is respectively observed as higher moisture contents before the freezing front. For clay, on the contrary, before the freezing front the moisture content decreases and in the freezing part it increases. The moisture excess in freezing clay depends on some soil parameters, including contents of moisture and salts, as well as on the conditions of freezing.

Figure 6a shows experimental points for moisture flow from unfrozen to partly frozen domain at different initial NaCl concentrations, from 0 to 1.5 N for two different temperatures [Chuvilin, 1999; Chuvilin et al., 1998]. The respective calculated curves (Figure 6b) are in good agreement with the experiment results. Note a peak of moisture flow that can be explained with calculated curves (Figure 6c, d): the moisture flow driven by osmosis is proportional to water saturation and to the magnitude of the concentration gradient. As the initial salinity increases, the former function increases while the latter modulo decreases (Figure 6c, d), and their product has a maximum and allows calculating the optimal salt concentration providing the maximum flow.

Calculations have shown that without the significant role of the osmotic effect, it is impossible to obtain a close description of the experiments. In [Chuvilin, 1999; Chuvilin et al., 1998], the important role of advection is noted in physical experiments, partially shown in Figures 5, 6. This study showed that the driving mechanism of this advection in the case of the solution being drawn into the frozen part is precisely the osmotic effect.

At the end of this section, we note that under certain conditions, the process under consideration can lead to the formation of closed “pockets” with brines (cryopegs) in frozen rocks. A mathematical criterion for their formation based on the proposed model was obtained in [Ramazanov et al., 2023].

6. Conclusion

The process of freezing of saline soil has been investigated with regard to the osmosis effect using the previously suggested model [Ramazanov et al., 2023], and an approximate analytical solution was obtained in the self-similarity formulation. In addition, a direct numerical solution has been obtained for large numbers of Péclet. The results demonstrate a good agreement between them.

It has been shown that at high values of the osmotic coefficient in freezing soils, the pore solution is drawn into the freezing domain from the thawed domain, and at low values, it is pushed out, on the contrary. The pushing force is due to the fact that the equilibrium pressure increases with decreasing temperature, as well as the density difference between water and ice. The modeling results are quite consistent with the data of physical experiments that clay with a high osmotic coefficient retract saline solutions, and sand, on the contrary, pushes it out [Chuvilin, 1999; Chuvilin et al., 1998]. The results of calculations and physical experiments agree both qualitatively and quantitatively, mainly because the osmotic effect was taken into account: no agreement would be possible otherwise.

The suggested mathematical model, with regard to osmosis, can explain freezing of soils as well as the reverse process of permafrost degradation.

Acknowledgments. This research, in general, was funded by the Russian Science Foundation, grant No. 22-67-00025.

References

- Berry, F. A. F., and B. B. Hanshaw (1960), Geologic evidence suggesting membrane properties of shales, in *International Geological Congress: report of the twenty-first session*, p. 209.
- Chuvilin, E. M. (1999), Migration of ions of chemical elements in freezing and frozen soils, *Polar Record*, 35(192), 59–66, <https://doi.org/10.1017/S0032247400026346>.

- Chuvilin, E. M., E. D. Ershov, and N. S. Naletova (1998), Mass transfer and structure formation in freezing saline soils, in *PERMAFROST - Seventh International Conference (Proceedings), Yellowknife (Canada), Collection Nordicana No 55*, Centre d'études nordiques, Université Laval.
- Chuvilin, E. M., V. Ekimova, B. Bukhanov, et al. (2019), Role of Salt Migration in Destabilization of Intra Permafrost Hydrates in the Arctic Shelf: Experimental Modeling, *Geosciences*, 9(4), 188, <https://doi.org/10.3390/geosciences9040188>.
- Dubikov, G. I., and N. V. Ivanova (1990), Saline frozen soils and their distribution in the USSR territory, in *Saline Frozen Soils as Foundations*, pp. 3–9, Nauka, Moscow (in Russian).
- Ershov, E. D., I. A. Komarov, and E. M. Chuvilin (1997), Forecast for interaction of liquid technogenous brines buried into permafrost, *Geokologiya*, (2), 19–29 (in Russian).
- Kemper, W. D. (1961), Movement of Water as Effected by Free Energy and Pressure Gradients: II. Experimental Analysis of Porous Systems in Which Free Energy and Pressure Gradients Act in Opposite Directions, *Soil Science Society of America Journal*, 25(4), 260–265, <https://doi.org/10.2136/sssaj1961.03615995002500040010x>.
- Lobkovskii, L. I., and M. M. Ramazanov (2018), Front Regime of Heat and Mass Transfer in a Gas Hydrate Reservoir under the Negative Temperature Conditions, *Fluid Dynamics*, 53(4), 517–530, <https://doi.org/10.1134/S0015462818040092>.
- Maksimov, A. M., and G. G. Tsypkin (1987), Overheating and formation of a two-phase zone at phase transitions in permafrost, *DAN USSR*, 294(5), 1117–1121 (in Russian).
- Marine, I. W., and S. J. Fritz (1981), Osmotic model to explain anomalous hydraulic heads, *Water Resources Research*, 17(1), 73–82, <https://doi.org/10.1029/WR017I001P00073>.
- Neuzil, C. E. (2000), Osmotic generation of 'anomalous' fluid pressures in geological environments, *Nature*, 403(6766), 182–184, <https://doi.org/10.1038/35003174>.
- Ramazanov, M. M., A. V. Karakin, and L. I. Lobkovskiy (2019), Mathematical Model for the Motion of Solutions Taking into Account the Osmotic Effect, *Doklady Earth Sciences*, 489(1), 1306–1309, <https://doi.org/10.1134/S1028334X19110060>.
- Ramazanov, M. M., N. S. Bulgakova, and L. I. Lobkovskiy (2022), Osmotic Convection, *Doklady Physics*, 67(5), 153–158, <https://doi.org/10.1134/S1028335822040061>.
- Ramazanov, M. M., N. Bulgakova, and L. Lobkovsky (2023), Mathematical Model of Freezing of Rocks Saturated With Salt Solution Taking Into Account the Influence of Osmosis, *Russian Journal of Earth Sciences*, 23(5), 1–15, <https://doi.org/10.2205/2023ES000857>.
- Shakhova, N., I. Semiletov, O. Gustafsson, et al. (2017), Current rates and mechanisms of subsea permafrost degradation in the East Siberian Arctic Shelf, *Nature Communications*, 8(1), <https://doi.org/10.1038/ncomms15872>.
- Streletskaia, I. D., and M. O. Leibman (2002), Cryogeochemical interrelation of massive ground ice, cryopegs, and enclosing deposits of central Yamal, *Kriosfera Zemli*, VI(3), 15–24 (in Russian), EDN: PWYRFB.
- Tsypkin, G. G. (2009), *Flows with Phase Transitions in Porous Media*, 232 pp., Fizmatlit (in Russian).
- Vasiliev, V. I., A. M. Maksimov, E. E. Petrov, and G. G. Tsypkin (1996), *Heat and Mass Transfer in Freezing and Thawing Soils*, 224 pp., Fizmatlit, Nauka, Moscow (in Russian).
- Yakushev, V. S. (2009), *Natural Gas and Gas Hydrate in Permafrost*, 190 pp., VNIIGAZ, Moscow (in Russian), EDN: OTRYFK.